Scientific Reports

https://doi.org/10.1038/s41598-026-55394-z

Article in Press

Effect of Muller maneuver on upper airway characteristics and surrounding structures in patients with obstructive sleep apnea: a cone-beam computed tomography study

Received: 14 September 2025

Accepted: 24 May 2026

Published online: 01 June 2026

Cite this article as: Arianezhad S.M., Safi Y., Ahsaie M.G. *et al.* Effect of Muller maneuver on upper airway characteristics and surrounding structures in patients with obstructive sleep apnea: a cone-beam computed tomography study. *Sci Rep* (2026). https://doi.org/10.1038/s41598-026-55394-z

S. Marjan Arianezhad, Yaser Safi, Mitra Ghazizadeh Ahsaie, Hamed Mortazavi & Seyed Sasan Aryanezhad

Effect of Muller maneuver on upper airway characteristics and surrounding structures in patients with obstructive sleep apnea: A cone-beam computed tomography study

Running title: Muller Maneuver effect in OSA patients using CBCT

Authors:

S. Marjan Arianezhad[1], Yaser Safi [2], Mitra Ghazizadeh Ahsaie[3], Hamed Mortazavi[4], Seyed Sasan Aryanezhad[5*]

1- Assistant professor, Department of Oral and Maxillofacial Radiology, School of Dentistry, Shahed University of Medical Sciences, Tehran, Iran marjan.arianezhad@gmail.com

2- Full Professor, Department of Oral and Maxillofacial Radiology, School of Dentistry, Shahid Beheshti University of Medical Sciences, Tehran, Iran dr.yaser.safi78@gmail.com

3- Assistant professor, Department of Oral and Maxillofacial Radiology, School of Dentistry, Shahid Beheshti University of Medical Sciences, Tehran, Iran mitraghazizadeh@gmail.com

4- Associate Professor, Department of Oral Medicine, School of Dentistry, Shahid Beheshti University of Medical Sciences, Tehran, Iran hamedmortazavi2013@gmail.com

5- Oral and Maxillofacial Radiologist, Department of Oral and Maxillofacial Radiology, school of Dentistry, Islamic Azad university of Isfahan (Khorasgan), Isfahan, Iran ariasasan7@gmail.com

***Corresponding author:** Seyed Sasan Aryanezhad **Email**: Ariasasan7@gmail.com

***Address correspondence to**: School of dentistry, Islamic Azad University of Isfahan (Khorasgan), Isfahan, Iran. Phone: +989122002527 ORCID *0000-0001-9851-1914*

Total number of pages: 26 Total number of figures: 6 Total number of tables: 4

Abstract

The Muller maneuver (MM) collapses the upper airway and mimics apneic events during sleep. This study aimed to assess the effect of MM on the upper airway (UA) and surrounding structures of patients with OSA using cone-beam computed tomography (CBCT). This prospective study of 18 moderate-to-severe OSA patients included two CBCT scans, one during gentle breathing and another while performing MM, with standardized head and neck positioning. UA , soft tissue, and hyoid bone were analyzed using linear, area, and volumetric measurements with OnDemand 3D software version 10.0.1 (1008 measurements). Paired t-tests, Wilcoxon signed-rank tests, Marginal Homogeneity tests, and two-way repeated-measures ANOVA were performed using SPSS version 27 software. Effect sizes were calculated using Cohen's d. MM statistically significantly decreased the following airway parameters: minimum anterior-posterior (mAP) of nasopharynx (6.41% (P=0.048)), mAP-oropharynx (38.81% (P=0.006)), minimum transverse(mT) of oropharynx (38.88% (P=0.006)), minimum cross-sectional area(mCSA) of oropharynx (42.02%; P=0.011), volume(V) of oropharynx (27.41% ;P=0.002), mAP-hypopharynx (19.77%;P=0.039) and mCSA-hypopharynx (11.77%;P=0.048), V-UA (11.76%;P=0.048) and minimum axial area (39.01%; P=0.007). MM also resulted in significant vertical hyoid bone changes and soft tissue length (P=0.001, P=0.016, respectively). Effect size analysis demonstrated predominantly moderate-to-large effects across variables, particularly for hyoid bone displacement and oropharyngeal airway narrowing, indicating that the observed changes were not only statistically significant but also clinically meaningful. This noninvasive, low-cost approach, provides comprehensive evaluation of the UA and surrounding

structures. It also offers functional insight by capturing airway configuration under negative pressure conditions, enabling a more dynamic assessment of airway behavior and collapsibility.

Keywords: Cone-beam computed tomography; Obstructive Sleep Apnea; Sleep apnea; Upper airway dimensions

Background

Obstructive sleep apnea (OSA) is a prevalent sleep-related breathing disorder characterized by the collapse of the tongue and soft tissue in the esophagus, causing airway obstruction during sleep. If left undiagnosed, OSA can be life-threatening[1]. OSA is associated with a reduction in quality of life and adverse health consequences such as hypertension, heart failure, myocardial infarction, stroke, and diabetes mellitus[2,3].

Several imaging modalities have been proposed for airway assessment[1,4]. However, each technique has its limitations, and a consensus on the gold standard has not yet been reached [5,6]. Three-dimensional (3D) imaging such as multi-detector computed tomography (MDCT) and magnetic resonance imaging (MRI) have been introduced but have several limitations. MRI has noisy scans and a claustrophobic effect, while MDCT has high radiation. Both are expensive, lack a dedicated sleep chamber, and require long scan times. Cone-beam computed tomography (CBCT) fits this gap perfectly because of its advantages in short scanning time and relatively low dose of radiation compared with MDCT[7,8]. Since the airway is a region of no attenuation, its boundaries are accurately detected in CBCT[9,10]. By utilizing a large field of view (FOV) protocol, CBCT provides a comprehensive 3D

inspection of the upper airway (UA) at various sections, making it a valuable modality for airway evaluation [5].

The Muller maneuver (MM), first suggested by Borowiecki and Sassin[11], simulates UA collapse during sleep under intraluminal pressure while the patient is awake. It is a forced inspiratory effort with the mouth closed and the nose occluded. MM is typically performed using a fiberoptic nasopharyngoscope to aid in the assessment of the degree and level of UA narrowing and has predictive value for OSA surgery[12]. However, the use of a fiberoptic nasopharyngoscope is relatively invasive and physician-subjective and cannot quantify the changes in surrounding structures (i.e., the soft palate, tongue, hyoid bone, and pharyngeal walls)[13,14].

The size of the UA and its ability to withstand intraluminal negative pressure are key factors in the pathophysiology of OSA[5]. Accordingly, precise identification of the site of obstruction is essential for treatment planning, selection of the optimal surgical approach, and assessment of prognosis and follow-up protocols[15]. Furthermore, as UA dimensions vary with patient positioning during imaging[5,6], assessment under different functional states and comparison of corresponding changes is necessary to capture clinically relevant changes[16,17]. Despite these difference, studies examining dynamic or functional alterations of the UA remain limited[12,18,19].

Therefore, this study aimed to be among the first to assess the effect of the MM on the characteristics of the UA and its surrounding structures in patients with OSA using CBCT.

Materials and methods

Ethics approval

This study was conducted in accordance with the principles of the Declaration of Helsinki. The study protocol was approved by the ethics committee of the university (IR.SBMU.DRC.REC.1402.076).

The institution's policy includes patients' consent to participate in any trial and approvals of using their data with full clarification of the benefits and risks of any procedure. CBCT scans were requested by the clinician for diagnostic process (and not for research purposes). No additional radiation dose was imposed on any subjects during the process. All patients' data were anonymized, and medical records were used solely for research purposes.

Study design and setting

There is currently no consensus on patient positioning during UA imaging[20,21], highlighting the need for a standardized approach. This prospective study included patients diagnosed with moderate-to-severe OSA based on clinical evaluation and polysomnography at the Sleep Department of Iran University, between January 2024 and July 2025. They were referred to the Oral and Maxillofacial Radiology Department at the School of Dentistry, Shahid Beheshti University of Medical Sciences for CBCT imaging.

Participants and eligibility criteria

The sample size was calculated to be 18 patients according to previous studies[22–26] assuming a 95% confidence interval, 80% study power, α=0.05, and β=0.2. Strict eligibility criteria were applied to minimize potential confounding factors.

The inclusion criteria were as follows:[27,28]

Dentate patients over 18 years, confirmed diagnosis of moderate (Apnea-Hypopnea Index (AHI) =15-20, and Respiratory Disturbance Index (RDI)=15-30) to severe (AHI > 30, respiratory disturbance index > 30) OSA by polysomnography results

The exclusion criteria were as follows:[19,29,30]

(1) Craniofacial anomalies, syndromic patients; (2) positive history of pharyngeal or orthognathic surgery, conditions with mandibular, pharyngeal, oral, and nasal involvements; (3) serious life-threatening diseases such as chronic obstructive pulmonary disease, symptomatic ischemic heart disease, congestive heart failure, cerebrovascular accident, chronic renal failure, and hypothyroidism; (4) history of asthma or sinusitis, diseases associated with airway inflammation such as the common cold and influenza; (5) pregnancy and nursing; (6) patients with psychiatric or neuromuscular conditions; (7) rheumatological diseases; (8) patients using intraoral appliances; (9) images with poor quality due to patient movement and artifacts, inadequate FOV.

CBCT Acquisition

Each patient underwent two CBCT scans by the same operator, using the same CBCT scanner (NewTom VGi, Verona, Italy) and consistent exposure settings, including a 300-µm voxel size, 15×15 FOV, variable tube current (mA), and 110 kVp. The first CBCT was performed during gentle breathing, with the lips closed, the tongue in a relaxed position, and the teeth in maximum intercuspation[31]. The second scan was acquired with the MM[13,19]. Participants were instructed to inhale forcefully with both their mouth and nostrils closed and were allowed to practice MM until they were comfortable performing it, in order to minimize variability and avoid repeated exposures. To improve standardization of the MM, all participants received uniform instructions and training before scanning. A nasal clip was applied immediately prior to exposure to ensure complete nasal occlusion, and correct mouth closure and patient posture was verified on the scout view. Additionally, participants were instructed to avoid swallowing or movement and to maintain stability throughout image acquisition. Head position was standardized for both scans to ensure consistent airway assessment and reduce variability. The scans were taken with the patients upright, the head in a natural position, and the horizontal visual axis, as per Solow and Tallgren[32]. The median plane aligned with the scanner's midface laser, minimizing tilt and rotation via laser lights and bilateral ear rods[33]. The two CBCT scans were obtained approximately two weeks apart and were prescribed by the clinicians for diagnostic purposes, and not for research purposes. The first scan was performed to evaluate the paranasal

sinuses and exclude potential pathologies, while the second scan was acquired preoperatively for airway assessment. All imaging procedures were conducted in accordance with the ALARA (As Low As Reasonably Achievable) principle, ensuring that radiation exposure was clinically justified and performed only when the expected diagnostic benefit outweighed potential risk. Moreover, CBCT was considered appropriate for this purpose due to its substantially lower radiation dose compared with conventional CT[21,34].

Image Processing

For interpretation, real time reconstruction was performed using On Demand 3D Application; Version 10.0.1 (Cybermed, Seoul, Korea). On the multiplanar reconstruction (MPR) screen, data were evaluated in axial, coronal, and sagittal planes and the voxels were isotropic[10]. CBCT images were displayed on a 21.3-inch flat panel, color active matrix and thin-film transistor medical monitor with 2048 × 2560 resolution, 11.9 bits, and 75 Hz (NEC MultiSync, Munich, Germany). Examiners were allowed to adjust image contrast and brightness to ensure optimal visualization. To minimize examiner fatigue, evaluations were conducted in multiple sessions throughout the day, and images were presented in a randomized order. Head orientation was standardized during image acquisition and subsequently re-evaluated and calibrated during image processing to ensure consistency and reproducibility across all measurements. The images were saved in DICOM (Digital Imaging and Communications in

Medicine) format and subsequently imported into OnDemand software for analysis by an experienced oral and maxillofacial radiologist, who was blinded to the study. Head position calibration was performed as follows: (1) coronal plane: the reference line was aligned with the bilateral infraorbital margins; (2) sagittal plane: horizontal calibration was established using the right infraorbital margin and the superior point of the right bony external auditory canal; and (3) horizontal plane: 3D skull repositioning was achieved using the nasion and sella turcica to establish a unified measurement baseline.

Image Analysis and Measurements

To perform measurements, anatomical landmarks were defined as described in Table 1 [10,35] and illustrated in Figure 1. Based on these landmarks, linear, area, and volumetric measurements were performed, as presented in Table 2 and illustrated in Figure 2 and 3.

A total of 1008 measurements were conducted, including evaluations of hyoid bone position [vertical measurements: HH1 and HH2, representing perpendicular distances from the hyoid to the mandibular and RGN–C3ia reference planes, respectively, and their sum (HH1+HH2); and horizontal measurements: H-C3ia and H-RGN, representing anteroposterior distances to cervical and mandibular landmarks], soft tissue parameters [posterior nasal spine to uvula distance (PNS–U) and soft palate maximum thickness (SP-max)], tongue dimensions and position [tongue length (TGL) and tongue

height (TGH)][36], and airway assessments (linear, area, and volumetric), as detailed in Tables 1 and 2.

Airway Segmentation and Analysis

The airway was divided into three subregions, as defined in Table 2. To assess airway morphology, the narrowest segment of each subregion was identified in the sagittal section and confirmed in the coronal and axial sections (Fig. 3). The cross-sectional area (mCSA), anterior-posterior dimension (mAP), and transverse dimension (mT) were measured (Table 1). Additionally, the mAP/mT ratio was calculated to evaluate airway shape. The smallest mCSA value across all subregions was recorded as the minimum axial area (MAA) in square millimeters (mm^2), along with its corresponding location (MAA location) [37,38]. The total airway dimensions were measured as the volume of the upper airway (V-UA), as described in Table 2.

Statistical analysis

The normality of the data distribution was analyzed by the Shapiro-Wilk test. Normally-distributed data were analyzed by paired t-test, whereas nonnormally distributed data were analyzed by the Wilcoxon signed rank test to assess the effect of the MM. A comparison of MAA before and after the MM was performed by the marginal homogeneity test. All the statistical analyses were performed using SPSS version 27 (SPSS Inc., IL, USA) at the 0.05 level of significance.

Effect sizes were calculated using Cohen's d to assess the magnitude of changes. Cohen's d was defined as the mean difference divided by the standard deviation of the differences. Effect sizes were interpreted as small (0.2), moderate (0.5), and large (≥0.8)[39,40].

To assess measurement reliability, 30% of the sample was randomly selected and re-evaluated. Intra-observer reliability was determined by repeating all measurements on the selected subset after a two-week interval by the same examiner. Inter-observer reliability was assessed by a second independent examiner who was blinded to the initial measurements and followed the same protocol. For continuous variables, intraclass correlation coefficients (ICC) were calculated using a two-way mixed-effects model (absolute agreement). For the categorical variable (MAA location), Cohen's kappa (κ) coefficient was used to assess both intra- and inter-observer agreement. ICC values were interpreted as poor (<0.50), moderate (0.50–0.75), good (0.75–0.90), and excellent (>0.90). Kappa values were interpreted as slight (<0.20), fair (0.21–0.40), moderate (0.41–0.60), substantial (0.61–0.80), and almost perfect (0.81–1.00).

Results

Reliability Analysis

Reliability analysis demonstrated excellent agreement for all continuous measurements. Intra-observer reliability showed ICC values ranging from 0.88 to 0.96, while inter-observer reliability showed ICC values ranging from 0.89 to 0.95. For the categorical variable (MAA location), intra-

observer agreement was almost perfect (κ = 0.84), whereas inter-observer agreement was substantial (κ = 0.73).

CBCT Measurement Analysis

Performing MM statistically significantly decreased the following airway parameters in CBCT: HH1, HH2, HH1+HH2, H-GRN, PNS-U, V-oropharynx, V-airway, AP-nasopharynx, mCSA-oropharynx, mAP-oropharynx, mT-oropharynx, mCSA-hypopharynx, mAP hypopharynx, and MAA ($P<0.05$), as presented in Table 3. MM had no significant effect on the other variables ($P>0.05$).

In the hyoid bone, MM caused 27.43% reduction in HH1 (P=0.002), 37.09% in HH2 (P<0.001), 31.81% in HH1 + HH2 (P=0.001), and 5.07% in H-RGN (P=0.031), indicating that the MM affected both the vertical and horizontal positions of the hyoid bone, with a greater effect on its vertical position.

In the soft tissue, the MM significantly reduced PNS-U by 7.51%. (P=0.016) meaning that the length of the posterior soft tissue decreased statistically significantly when the MM was performed, but it did not have a significant effect on the thickness of the soft tissue or the dimensions of the tongue.

In the nasopharynx, the mAP decreased by 6.41% (P=0.048). In the oropharynx, performing the MM resulted in significant decreases: in mAP by 38.81% (P=0.006), mT by 38.88% (P=0.006), mCSA by 42.02% (P=0.011), and volume by 27.41% (P=0.002). In the hypopharynx, MM decreased the mAP and mCSA by 19.77% (P=0.039) and 11.77% (P=0.048), respectively. The V-UA decreased by 11.76% (P=0.048), and the MAA

decreased by 39.01% (P=0.007) when the MM was performed. Figure 4 shows sagittal and axial CBCT images of a patient while performing MM. In summary, MM caused a statistically significant reduction in the mAP across all 3 subregions of the airway. For mT, a significant reduction was observed only in the oropharynx. The mCSA significantly decreased in both the oropharynx and hypopharynx due to MM. Additionally, the V-oropharynx and V-UA, as well as the MAA, were significantly reduced by MM as shown in Fig. 5.

The MAA location was in the oropharynx in most subjects on both CBCT scans with/without the MM. The marginal homogeneity test revealed that the MM had no significant effect on the location of MAA (P=0.366).

For mAP/mT ratios, a value close to 1 indicates a circular airway. Ratios greater than 1 suggest an elliptical airway with a larger anterior-posterior dimension, whereas ratios less than 1 indicate an elliptical airway with a larger transverse dimension. A one-sample test of mAP/mT ratios revealed that, both with and without the MM, the overall shape of the airway in all three subregions was elliptical, with a larger mT exceeding mAP (ratio < 1). This ratio was not significantly affected by the MM, and the airway shape remained elliptical (P>0.05).

Effect size analysis

Table 4 presents the descriptive statistics and effect sizes (Cohen's *d*) for measured variables showing statistically significant changes. Overall, the effect size analysis demonstrated predominantly moderate to large effects

across variables, indicating that the MM induced meaningful changes in hyoid bone position, posterior soft tissue and UA. Large effect sizes were observed for changes in HH1 ($d = 0.98$), HH2 ($d = 1.35$), and the combined HH1+HH2 ($d = 1.25$), indicating substantial vertical displacement of the hyoid bone during the MM. Moderate-to-large effect sizes were also found for oropharyngeal airway parameters, including mCSA, mAP, and mT (approximately $d = 0.70–0.74$), suggesting clinically relevant narrowing of the oropharyngeal airway during the MM.

The MAA showed a moderate effect size ($d = 0.60$), indicating a meaningful reduction in the narrowest overall airway dimension. Similarly, posterior soft tissue length and V-UA showed a moderate effect ($d = 0.66$, $d = 0.51$, respectively). In contrast, smaller effect sizes were observed in the nasopharynx and hypopharynx (mCSA-hypopharynx $d = 0.19$), suggesting more limited changes in these regions.

Discussion

To the best of the authors' knowledge, this study is one of the first to assess the effect of the MM on the UA and surrounding structures using CBCT scans acquired in patients with OSA, providing a comprehensive 3D evaluation of hyoid bone, soft tissue, UA and its sub regions in terms of linear, area, volumetric, and morphological characteristics.

The use of CBCT with MM offers several advantages. In contrast to fiberoptic endoscopy with MM, which is an invasive procedure and provides limited information regarding the exact site of airway narrowing[13,41], CBCT

with MM is noninvasive and allows for dynamic, 3D evaluation of UA morphology and surrounding structures, providing significantly more information than nasopharyngoscopy. Additionally, CBCT is considered the gold standard for angular and linear measurements[30]. Compared to MDCT, it offers a lower radiation dose and shorter acquisition time, which facilitates the implementation of the MM. As patients cannot undergo imaging while asleep, and the dynamic airway changes that occur over the course of sleep are not captured, no imaging modality can fully replicate the natural sleep state. The application of the MM during CBCT acquisition provides functional imaging by replicating this state.

In the present study, the best effort was made to use a restricted methodology to minimize confounding factors. Firstly, to reduce postural variability and ensure consistency across scans, CBCT acquisition was standardized using the same positioning protocol, operator, and imaging unit. Secondly, head orientation was re-evaluated and calibrated during image processing to ensure reproducibility and reduce measurement error. Thirdly, to address the variability in airway landmark definitions reported in the literature[42], hard tissue landmarks were used to delineate airway boundaries, providing greater precision and consistency compared to soft tissue references[10]. Finally, effect sizes were used to evaluate the clinical relevance of changes induced by the MM. Reporting effect sizes complements P-values by providing information on the practical significance of the findings. Our results indicate that the MM not only affects airway

dimensions but also induces substantial changes in vertical hyoid position and posterior soft tissue length.

The MAA and mCSA which are strongly associated with the pathogenesis of OSA[19] were analyzed in our study. The narrowest part of the UA was consistently located in the oropharynx, both with and without the MM, which was in line with previous findings[6,16]. This predisposition of the oropharynx to obstruction may be due to its high susceptibility to collapse.. This region also exhibited moderate-to-large effect sizes induced by the MM, highlighting the value of the MM in enhancing the detection of potential sites of obstruction and providing additional information through dynamic airway evaluation. From a clinical perspective, precise identification of both the location and extent of airway narrowing is essential for appropriate surgical candidate selection and procedure planning. Accordingly, these findings assist clinicians in optimizing treatment decisions and planning. Our findings are in line with the study of Arora et al.[12] who reported obstruction found on CT during MM significantly correlated with DISE results in the velum and base of the tongue. The MM resulted in a significant reduction in the mAP of all three sub regions, whereas the mT was significantly reduced only in the oropharynx, highlighting the substantial impact of MM on the AP dimension of the UA. Huang et al. [19] reported that the mCSA-oropharynx and hypopharynx had an inverse association with the severity of OSA when the MM was performed during CT, but mCSA-nasopharynx was an independent

variable in OSA patients. Similarly, in this study, significant changes in mCSA were observed in the oropharynx and hypopharynx, but not in the nasopharynx.

The airway shape in all three subregions was elliptical with a mT greater than mAP both with and without the MM, which was consistent with the results of Wu et al.[43], and Ogawa et al.[44], and in contrast to the findings of Huang et al.[19], who reported a more circular shape in the nasopharynx and oropharynx. This discrepancy may be due to the use of different imaging modalities, patient positioning in the scanner, and different eligibility criteria.

In this study, performing MM resulted in statistically significant vertical displacement of the hyoid bone, with a large effect size during the MM. Sobouti et al.[45] reported that the vertical position of the hyoid bone significantly influences OSA severity. The present findings are consistent with those of Sobouti et al. Accordingly, we suggest that the observed displacement during MM may reflect functionally relevant changes associated with airway collapsibility. Our study also demonstrated a decrease in the length of posterior soft tissues with a moderate effect size. These findings contrast with those of Liao et al.[27], who reported posterior and downward displacement of the tongue and hyoid bone during MM, along with alterations in tongue shape. However, their analysis was based on two-dimensional cephalometric imaging, which has inherent limitations in the evaluation of 3D structures. In contrast, the present study utilized

CBCT, allowing for a more accurate 3D assessment of the UA and its surrounding structures during the MM.

There is currently no consensus on patient positioning during UA imaging, and a standardized approach is lacking[20,21]. In addition, UA dimensions are influenced by patient positioning and functional status during imaging. Therefore, it is important to evaluate the UA under different dynamic conditions and compare the resulting changes. As most imaging modalities assess the airway in a static state, they may not fully reflect its functional behavior. As a result, CBCT imaging performed during the MM may serve as a noninvasive functional adjunct to conventional static assessment, potentially providing additional insight into airway dynamics. Compared with CBCT performed under static conditions, this approach offers functional information by capturing airway configuration under negative pressure conditions. From a clinical perspective, it may serve as a complementary tool in preoperative evaluation, assisting clinicians in understanding patient-specific patterns of airway narrowing. Furthermore, integrating MM-CBCT findings into clinical decision-making may support a more personalized approach to OSA management by enabling treatment selection based on three-dimensional patterns of airway collapse rather than severity alone.

The present study has some limitations. Firstly, the relatively small sample size was due to the strict eligibility criteria. Secondly, the limited number of comparable studies restricted direct comparisons with existing literature.

Thirdly, the inspiratory pressure generated with the MM was not quantified for each patient as the MM was performed based on standardized patient instructions, reflecting common clinical practice. Future studies incorporating objective pressure monitoring or graded inspiratory efforts are recommended. Finally, CBCT was used for the evaluation of soft tissue measurements. Although MDCT is considered the gold standard for soft tissue imaging, CBCT was selected due to its lower radiation dose and greater accessibility[4,6]. CBCT has been widely used in recent studies for craniofacial assessment[4,45] and has been shown to provide clinically acceptable accuracy for soft tissue measurements, particularly when overall dimensions rather than detailed tissue differentiation are required, as in the present study[7,9]. Correlating the site of airway obstruction identified by this method with intraoperative findings, as well as studies with larger sample sizes, could further validate its clinical applicability. By addressing these recommendations, the field can advance toward more effective OSA management strategies by advanced imaging techniques, facilitating early intervention and improving patient outcomes.

Conclusion

MM induced the statistically significant changes in the oropharynx, followed by the hypopharynx and nasopharynx, with significant effects on the hyoid bone and soft palate. CBCT with MM, as a noninvasive, low-cost, and low-radiation 3D imaging modality, provides comprehensive information about the dimensions of the UA and its surrounding structures. This approach

provides additional functional insight by capturing airway configuration under negative pressure conditions, thereby enabling a more dynamic and functional assessment of airway behavior and collapsibility rather than a static evaluation. Therefore, it assists clinicians in accurately and efficiently identifying potential sites of airway obstruction. In addition to other diagnostic approaches, it may contribute to effective treatment planning for OSA, enable early intervention, and improve surgical outcomes.

Abbreviations:

OSA – Obstructive sleep apnea

3D – Three-dimensional

MDCT – Multi-detector computed tomography

MRI – Magnetic resonance imaging

FOV – Field of view

FHP – Frankfort horizontal plane

UA: Upper airway

MM : Muller maneuver

AHI: Apnea-Hypopnea Index

RDI: Respiratory Disturbance Index

RGN – Retrognathion

HH1, HH2 – Vertical hyoid position measurements

PNS–U – Posterior nasal spine–uvula distance

SP-max – Maximum thickness of the soft palate

TGH – Tongue height

TGL – Tongue length

mAP – Minimum anteroposterior dimension

mT – Minimum transverse dimension

mAP/mT – Ratio of minimum anterior posterior to minimum transverse

mCSA – Minimum cross-sectional area

CSA – cross-sectional area

MAA – Minimum axial area

UA – Upper airway

V-UA – Volume of the upper airway

V-subregion – Volume of airway subregions (nasopharynx, oropharynx, hypopharynx)

DICOM – Digital imaging and communications in medicine

ICC – Intraclass correlation coefficient

Declarations

ethics approval and consent to participant: This study was performed in line with the principles of the Declaration of Helsinki. Approval was granted by the Ethics Committee Shahid Beheshti University of Medical Sciences (IR.SBMU.DRC.REC.1402.076).

Consent for publication: Not applicable

Availability of data and materials: The data that support the findings of this study are available from the corresponding author upon reasonable request.

Competing interests: The authors have no relevant financial or non-financial interest

Funding: The authors declare that no funds, grants, or other support were received during the preparation of this manuscript interests to disclose.

Authors' contributions: Y.S. implemented the study idea. M.GA. Provided CBCT data. H.M. provided statistical analysis. S.M.A. drafted the main manuscript. S.S.A. revised the manuscript.

Acknowledgments: Not applicable

Statements and Declarations: The authors also confirmed that the manuscript is original and does not contain any unlawful statements and any material, the publication of which would violate any copyright or other personal or proprietary right of any person or entity. They also confirm that they have written permission from copyright owners if their work has been used in this manuscript. The authors declare that the following manuscript has not been published elsewhere (in any format or language) and has not been concomitantly sent to another journal for publication consideration. The authors agree that they are responsible for paying any fees for permissions.

References:

1. Maspero, C., Giannini, L., Galbiati, G., Rosso, G. & Farronato, G. Obstructive sleep apnea syndrome: a literature review. *Minerva Stomatol* **64**, 97–109 (2015).

2. Kostrzewa-Janicka, J., Śliwiński, P., Wojda, M., Rolski, D. & Mierzwińska-Nastalska, E. Mandibular Advancement Appliance for Obstructive Sleep Apnea Treatment. *Adv Exp Med Biol* **944**, 63–71 (2017).
3. Borel, A. L. Sleep Apnea and Sleep Habits: Relationships with Metabolic Syndrome. *Nutrients* **11**, (2019).
4. Heriasti, M. D., Hariri, F. & Tay, H. W. Role of Cone-Beam Computed Tomography (CBCT) in Obstructive Sleep Apnea (OSA): A Comprehensive Review. *Diagnostics (Basel)* **16**, 298 (2026).
5. Paramasivan, V. K., Kishore, S., Agrawal, V. & Kameswaran, M. Radiological Diagnosis in OSA. in *Obstructive Sleep Apnea: A Multidisciplinary Approach* (eds Baptista, P. M., Lugo Saldaña, R. & Amado, S.) 369–393 (Springer International Publishing, Cham, 2023). doi:10.1007/978-3-031-35225-6_21.
6. Isaac, M., ElBeshlawy, D. M., ElSobki, A., Ahmed, D. F. & Kenawy, S. M. The role of cone-beam computed tomography in the radiographic evaluation of obstructive sleep apnea: A review article. *Imaging Sci Dent* **53**, 283–289 (2023).
7. Patcas, R. *et al.* Accuracy of linear intraoral measurements using cone beam CT and multidetector CT: a tale of two CTs. *Dentomaxillofacial Radiology* **41**, 637–644 (2012).
8. Valizadeh, S., Ghazizadeh Ahsaie, M., Ahmadvand, H. & Arianezhad, S. M. Anatomical Variations of the Canalis Sinuosus in the Anterior Maxilla: A Cone-Beam Computed Tomography Study. *I J Radiol* **22**, (2025).

9. Aflah, K. A., Yohana, W. & Oscandar, F. Volumetric measurement of the tongue and oral cavity with cone-beam computed tomography: A systematic review. *Imaging Sci Dent* **52**, 333 (2022).

10. Hashemi, S. Z. *et al.* Evaluation of pharyngeal airway volume, soft-tissue changes, and risk of obstructive sleep apnea after bimaxillary orthognathic surgery in patients with skeletal Class III malocclusion using cone-beam computed tomography and the STOP-BANG questionnaire: A long-term study. *American Journal of Orthodontics and Dentofacial Orthopedics* S0889540626001332 (2026) doi:10.1016/j.ajodo.2026.02.010.

11. Borowiecki, B. D. & Sassin, J. F. Surgical treatment of sleep apnea. *Arch Otolaryngol* **109**, 508–12 (1983).

12. Arora, K., Bansal, S., Jain, D., Gupta, V. & Virk, R. S. Comparing Diagnostic Efficacy of Imaging During Muller's Maneuver Versus Drug Induced Sleep Endoscopy in Obstructive Sleep Apnoea. *Indian J Otolaryngol Head Neck Surg* **75**, 624–631 (2023).

13. Terris, D. J., Hanasono, M. M. & Liu, Y. C. Reliability of the Muller maneuver and its association with sleep-disordered breathing. *Laryngoscope* **110**, 1819–23 (2000).

14. Zhou, X. *et al.* A Simple Method for Noninvasive Quantification of Pressure Gradient Across the Pulmonary Valve. *Sci Rep* **7**, 42745 (2017).

15. Sundaram, S., Bridgman, S. A., Lim, J. & Lasserson, T. J. Surgery for obstructive sleep apnoea. *Cochrane Database Syst Rev* Cd001004 (2005) doi:10.1002/14651858.CD001004.pub2.

16. Arslan, E. & Yazıcı, H. Obstructive Sleep Apnea: ENT Perspective. in *Airway diseases* (eds Cingi, C., Yorgancıoğlu, A., Bayar Muluk, N. & Cruz, A. A.) 1–12 (Springer International Publishing, Cham, 2023). doi:10.1007/978-3-031-22483-6_128-1.

17. Liu, Y. *et al.* Dynamic behavior of the oropharynx airway during deep breath in patients with obstructive sleep apnoea hypopnoea syndrome observed by ultrasonography. *Sci Rep* **15**, 5585 (2025).

18. Stanford, W., Galvin, J. & Rooholamini, M. Effects of awake tidal breathing, swallowing, nasal breathing, oral breathing and the Müller and Valsalva maneuvers on the dimensions of the upper airway. Evaluation by ultrafast computerized tomography. *Chest* **94**, 149–54 (1988).

19. Huang, J. F. *et al.* Assessment of Upper-Airway Configuration in Obstructive Sleep Apnea Syndrome With Computed Tomography Imaging During Müller Maneuver. *Respir Care* **61**, 1651–1658 (2016).

20. Alsufyani, N. A., Al-Saleh, M. A. & Major, P. W. CBCT assessment of upper airway changes and treatment outcomes of obstructive sleep apnoea: a systematic review. *Sleep Breath* **17**, 911–23 (2013).

21. Gurgel, M. L. *et al.* Methodological parameters for upper airway assessment by cone-beam computed tomography in adults with

obstructive sleep apnea: a systematic review of the literature and meta-analysis. *Sleep Breath* **27**, 1–30 (2023).

22. Borowiecki, B., Pollak, C. P., Weitzman, E. D., Rakoff, S. & Imperato, J. Fibro-optic study of pharyngeal airway during sleep in patients with hypersomnia obstructive sleep-apnea syndrome. *Laryngoscope* **88**, 1310–3 (1978).
23. Camacho, M., Capasso, R. & Schendel, S. Airway changes in obstructive sleep apnoea patients associated with a supine versus an upright position examined using cone beam computed tomography. *J Laryngol Otol* **128**, 824–30 (2014).
24. Romano, S. *et al.* Upper airway collapsibility evaluated by a negative expiratory pressure test in severe obstructive sleep apnea. *Clinics* **66**, 567–572 (2011).
25. Carrera, H. L. *et al.* Negative Expiratory Pressure Technique: An Awake Test to Measure Upper Airway Collapsibility in Adolescents. *Sleep* **38**, 1783–1791 (2015).
26. Huang, E. I., Lin, Y.-C., Huang, S.-Y., Lin, C.-K. & Lin, C.-M. Shifting and reducing breathing disturbance in patients with very severe obstructive sleep apnea by modified Z-palatoplasty with one-layer closure in one-stage multilevel surgery. *Sci Rep* **11**, 8472 (2021).
27. Liao, Y. F., Huang, C. S. & Chuang, M. L. The utility of cephalometry with the Muller maneuver in evaluating the upper airway and its

surrounding structures in Chinese patients with sleep-disordered breathing. *Laryngoscope* **113**, 614–9 (2003).

28. Sateia, M. J. International classification of sleep disorders-third edition: highlights and modifications. *Chest* **146**, 1387–1394 (2014).
29. Tikku, T. *et al.* Dimensional and volumetric analysis of the oropharyngeal region in obstructive sleep apnea patients: A cone beam computed tomography study. *Dent Res J (Isfahan)* **13**, 396–404 (2016).
30. Venza, N., Malara, A., Liguori, C., Cozza, P. & Laganà, G. Upper Airway Characteristics and Morphological Changes by Different MADs in OSA Adult Subjects Assessed by CBCT 3D Imaging. *Journal of Clinical Medicine* **12**, 5315 (2023).
31. Iwasaki, T. *et al.* Tongue posture improvement and pharyngeal airway enlargement as secondary effects of rapid maxillary expansion: A cone-beam computed tomography study. *American Journal of Orthodontics and Dentofacial Orthopedics* **143**, 235–245 (2013).
32. Solow, B. & Tallgren, A. Natural head position in standing subjects. *Acta Odontol Scand* **29**, 591–607 (1971).
33. Mageet, A., Khamis, A. & McDonald, J. Obstructive Sleep Apnoea Hypopnoea Syndrome and the Cranio Facio-hyoid Morphology in Adults: Linear and Angular Measurements. *International Journal of Clinical & Laboratory Research* **3**, 8 (2015).
34. Lam, E. W. N. & Mallya, S. M. *White and Pharoah's Oral Radiology Principles and Interpretation*. (2025).

35. Kim, H. Y., Bok, K. H., Dhong, H. J. & Chung, S. K. The correlation between pharyngeal narrowing and the severity of sleep-disordered breathing. *Otolaryngol Head Neck Surg* **138**, 289–93 (2008).

36. Tahmasbi, S., Bakhtiari, D., Dalaie, K., Safi, Y. & Eskandarloo, F. The Relation Between Posture and Dimension of Tongue and Different Sagittal Skeletal Patterns and Vertical Skeletal Patterns in Class I and Class II Patients: A CBCT Study. *International Journal of Dentistry* **2026**, 5529949 (2026).

37. Shi, X. *et al.* Upper airway morphology in adults with positional obstructive sleep apnea. *Sleep and Breathing* 1–9 (2023).

38. Shi, X. *et al.* Effects of mandibular advancement devices on upper airway dimensions in obstructive sleep apnea: responders versus non-responders. *Clin Oral Investig* **27**, 5649–5660 (2023).

39. Sullivan, G. M. & Feinn, R. Using Effect Size—or Why the P Value Is Not Enough. *Journal of Graduate Medical Education* **4**, 279–282 (2012).

40. Lakens, D. Calculating and reporting effect sizes to facilitate cumulative science: a practical primer for t-tests and ANOVAs. *Front. Psychol.* **4**, (2013).

41. Petri, N., Suadicani, P., Wildschiødtz, G. & Bjørn-Jørgensen, J. Predictive value of Müller maneuver, cephalometry and clinical features for the outcome of uvulopalatopharyngoplasty. Evaluation of predictive factors using discriminant analysis in 30 sleep apnea patients. *Acta Otolaryngol* **114**, 565–71 (1994).

42. Guijarro-Martínez, R. & Swennen, G. R. J. Cone-beam computerized tomography imaging and analysis of the upper airway: a systematic review of the literature. *International Journal of Oral and Maxillofacial Surgery* **40**, 1227–1237 (2011).

43. Wu, Q., Liu, H., Zhu, Z., Liu, L. & Luo, E. Characterization of upper airway and analysis of potential risk factor associated with OSA in patients with unilateral temporomandibular ankylosis and micrognathia deformities. *J Stomatol Oral Maxillofac Surg* **125**, 101708 (2023).

44. Ogawa, T., Enciso, R., Shintaku, W. H. & Clark, G. T. Evaluation of cross-section airway configuration of obstructive sleep apnea. *Oral Surg Oral Med Oral Pathol Oral Radiol Endod* **103**, 102–8 (2007).

45. Sobouti, F. *et al.* The relationship between clinical severity of obstructive sleep apnea based on polysomnography and drug-induced sleep endoscopy with 3D, 2D, linear, and angular anatomical parameters of upper airway and craniofacial area in CBCTs of individuals with moderate or severe apnea: a cross-sectional study. *Clin Oral Invest* **30**, 50 (2026).

Tables

Landmark	**Definition**
PNS	Posterior nasal spine: The tip of the posterior nasal spine
Me	Menton: The lower most point on the mandibular symphysis in the midline

Go	Gonion: The intersection of the line connecting the most distal aspect of the condyle to the distal border of the ramus and the mandibular plane
RGN	The most inferior-posterior point on the mandibular symphysis.
C3ia	The most inferior-anterior point of the body of the third cervical vertebra
C4ia	The most inferior-anterior point of the body of the fourth cervical vertebra
H	The upper edge of the frontal area of hyoid body
H1	Perpendicular from H to the mandibular plane (Go-Me)
H2	Perpendicular from H to the line RGN-cv3ia
Linear Measurements	**Definition**
FHP	Frankfurt horizontal plane: The line through point Or and Po.
MP	Mandibular plane: The line connecting Me to Go.
HH1	The linear distance along a perpendicular from hyoid (H) to the Mandibular plane: MPH
HH2	The linear distance between hyoid (H) and a perpendicular to the RGN-C3ia plane

HH1+HH2	Vertical hyoid position
H-C3ia	The linear distance between the hyoid (H) and the most inferior-anterior point of the body of the third cervical vertebra
H-RGN	The linear distance between hyoid (H) and retrognathion
PNS-U distance	The posterior nasal spine to the tip of the uvula, which provides a measure of the length of the soft palate.
SP-max	Maximum thickness of the soft palate perpendicular to PNS-U
TGL	Tongue length: the distance from epiglottis base and tongue tip
TGH	Tongue height: the length of the vertical bisector from the dorsal tongue surface to a line connecting between the epiglottis base and tongue tip
mAP	Minimum Anterior Posterior dimension: anteroposterior dimension of the narrowest segment of each subregion
mT	Minimum transverse dimension: transverse dimension of the narrowest segment of each subregion
L-UA	Length of upper airway: the vertical distance from the upper limit of the nasopharynx to the lower margin of the hypopharynx in the mid-sagittal plane
Area measurements	**Definition**

mCSA	Minimum cross-sectional area: cross sectional area of the narrowest segment of each subregion
Volumetric measurements	**Definition**
V-subregion	Volume of each subregion of airway: nasopharynx, oropharynx, hypopharynx
V-UA	volume of upper airway: total volume from the upper limit of the nasopharynx to the lower margin of the hypopharynx in the mid-sagittal plane.

Table 1. Definitions of anatomical landmarks, linear and volumetric measurements used in this study.

Region	**limits**	**Anatomical**	**Technical**
Nasopharynx	Anterior	Frontal plane perpendicular to FH passing through PNS	Same as anatomical
	Posterior	Soft tissue contour of the pharyngeal wall	Frontal plane perpendicular to FH passing through C2sp
	Upper	Soft tissue contour of the pharyngeal wall	Top of the upper airway: Plane parallel to FH passing through the last axial slice before the

			nasal septum fused with the posterior pharyngeal wall
	Lower	Plane parallel to FH passing through PNS and extended to the posterior wall of the pharynx	Same as anatomical
	Lateral	Soft tissue contour of the pharyngeal wall	Sagittal plane perpendicular to FH passing through the lateral walls of the maxillary sinus
Oropharynx	Anterior	Frontal plane perpendicular to FH passing through PNS	Same as anatomical
	Posterior	Soft tissue contour of the pharyngeal wall	Frontal plane perpendicular to FH passing through C2sp
	Upper	Lower limit of Nasopharynx	Same as anatomical
	Lower	Plane parallel to FH plane passing through C3ai	Same as anatomical

	Lateral	Soft tissue contour of the pharyngeal wall	Sagittal plane perpendicular to FH passing through the lateral walls of the maxillary sinus
Hypopharynx	Anterior	Frontal plane perpendicular to FH passing through PNS	Same as anatomical
	Posterior	Soft tissue contour of the pharyngeal wall	Frontal plane perpendicular to FH passing through C2ia
	Upper	Lower limit of Oropharynx	Same as anatomical
	Lower	Plane parallel to FH connecting the base of the epiglottis to the entrance to the esophagus	Plane parallel to FH connecting the base of the epiglottis to C4ai
	Lateral	Soft tissue contour of the pharyngeal wall	Sagittal plane perpendicular to FH passing through the lateral walls of the maxillary sinus
Upper airway	Anterior	Frontal plane perpendicular to FH passing through PNS	Same as anatomical

	Posterior	Soft tissue contour of the pharyngeal wall	Frontal plane perpendicular to FH passing through C2sp
	Upper	Soft tissue contour of the pharyngeal wall	Top of the upper airway: Plane parallel to FH passing through the last axial slice before the nasal septum fused with the posterior pharyngeal wall
	Lower	Plane parallel to FH connecting the base of the epiglottis to the entrance to the esophagus	Plane parallel to FH connecting the base of the epiglottis to C4ai
	Lateral	Soft tissue contour of the pharyngeal wall	Sagittal plane perpendicular to FH passing through the lateral walls of the maxillary sinus

Table 2. Definitions of anatomical boundaries and segmentation criteria used for airway measurements.

Variables (with/without MM)	Mean	Std. Deviation	Unit	P value

Pair 1	H-H1 +	13.1839	5.60066	mm	0.002*
	H-H1 -	18.8322	6.17667	mm	
Pair 2	H-H2 +	7.0383	3.28134	mm	<
	H-H2 -	12.2906	4.85505	mm	0.001*
Pair 3	(HH1+HH2) +	20.2222	8.33380	mm	0.001*
	(HH1+H2) -	31.1228	10.47617	mm	
Pair 4	H-C3 +	38.3706	4.13488	mm	0.202*
	H-C3 -	37.1861	3.49543	mm	
Pair 5	H-RGN+	41.0350	5.11893	mm	0.031*
	H-RGN -	43.6900	7.25449	mm	
Pair 6	PNS-U +	34.7756	5.77355	mm	0.016*
	PNS-U -	37.8944	6.19687	mm	
Pair 7	SP-max +	7.2094	1.67494	mm	0.061*
	SP-max -	8.18883	1.798669	mm	
Pair 8	TGL +	80.9406	7.56098	mm	0.454*
	TGL -	81.9422	5.28552	mm	
Pair 9	TGH +	39.4522	4.21773	mm	0.194*
	TGH -	40.9894	3.07323	mm	
Pair 10	V-nasopharynx +	4501.3711	1097.88522	mm^3	0.138*
	V-nasopharynx -	4758.8983	1253.12980	mm^3	
Pair 11	V-oropharynx +	5064.4333	2797.54536	mm^3	0.002†
	V-oropharynx -	9101.8544	8441.23895	mm^3	

Pair 12	V-hypopharynx+	6637.9000	2960.02871	mm^3	0.286†
	V-hypopharynx -	7227.1761	3093.65010	mm^3	
Pair 13	V-airway+	16792.9806	5937.45190	mm^3	0.048†
	V-airway-	20498.6528	9288.06575	mm^3	
Pair 14	mCSA nasopharynx+	161.5700	38.90478	mm^2	0.085†
	mCSA nasopharynx-	177.3828	55.28774	mm^2	
Pair 15	mAP-nasopharynx +	6.9606	2.18565	mm	0.048†
	mAP-nasopharynx -	7.5017	1.77169	mm	
Pair 16	mT-nasopharynx +	20.0572	2.73341	mm	0.995*
	mT-nasopharynx -	20.0594	2.63069	mm	
Pair 17	AP/T nasopharynx +	.3505	.11033	mm	0.214*
	AP/T nasopharynx -	.3766	.08166	mm	
Pair 18	mCSA oropharynx+	48.5422	45.42736	mm^2	0.011*
	mCSA oropharynx -	115.3822	77.16149	mm^2	
Pair 19	mAP-oropharynx +	3.9989	3.45455	mm	0.006*
	mAP-oropharynx -	6.7833	2.00536	mm	
Pair 20	mT-oropharynx +	8.9011	7.89603	mm	0.006*
	mT-oropharynx -	18.1906	7.50047	mm	
Pair 21	AP/T oropharynx +	.4059	.51180	mm	0.145†
	AP/T-oropharynx -	.4331	.21656	mm	

Pair 22	mCSA Hypopharynx +	180.1044	82.87810	mm²	0.048†
	mCSA Hypopharynx -	375.6239	588.32984	mm²	
Pair 23	mAP hypopharynx +	8.7106	4.43909	mm	0.039†
	mAP hypopharynx -	12.0417	3.78838	mm	
Pair 24	mT hypopharynx +	19.4922	9.74157	mm	0.070*
	mT hypopharynx -	25.0512	8.41106	mm	
Pair 25	AP/Thypopharynx +	.5380	.38627	mm	0.501†
	AP/T hypopharynx -	.5441	.30298	mm	
Pair 26	MAA in airway +	51.1344	51.81048	mm²	0.007†
	MAA in airway -	106.9567	50.10624	mm²	
Pair 27	Airway length +	89.1472	6.01096	mm	0.123*
	Airway Length -	89.8411	6.72913	mm	

Table 3. Comparison of variables obtained from CBCT images with and without the Muller maneuver.

Abbreviations: +, with Muller maneuver; -, without Muller maneuver; AP, Anteroposterior; T, transverse; AP/T, anteroposterior/transverse; V, volume; mCSA, minimum cross-sectional area; MAA, minimum axial area; * based on paired t-test; † based on Wilcoxon signed rank test

Variable	Minimum	Maximum	Mean	Std. Deviation	Cohen's d
H-H1 change	-75.08	19.90	-27.4352	27.90261	0.98
HH2 change	-78.84	6.14	-37.0960	27.52064	1.35
HH1+HH2 change	-76.60	11.05	-31.8108	25.39856	1.25
H-RGN change	-20.33	14.04	-5.0734	10.14688	0.50
PNS-U change	-33.54	8.99	-7.5154	11.39206	0.66

V-oropharynx change	-94.24	27.85	-27.4168	33.83232	0.81
V-airway change	-76.80	14.41	-11.7620	22.98114	0.51
mAP-nasopharynx change	-35.49	59.16	-6.4133	23.60183	0.27
mCSA-oropharynx change	-100.00	83.93	-42.0299	60.00345	0.70
mAP-oropharynx change	-100.00	79.30	-38.8182	52.94263	0.73
mT-oropharynx change	-100.00	40.90	-38.8803	52.72732	0.74
mCSA-hypopharynx change	-100.00	126.65	-11.7782	60.61004	0.19
mAP-hypopharynx change	-100.00	36.58	-19.7762	38.77550	0.51
MAA change	-100.00	93.07	-39.0139	64.65082	0.60

Table 4. Statistical measures and effect sizes for variables demonstrating statistically significant differences following the Muller maneuver.

Figures:

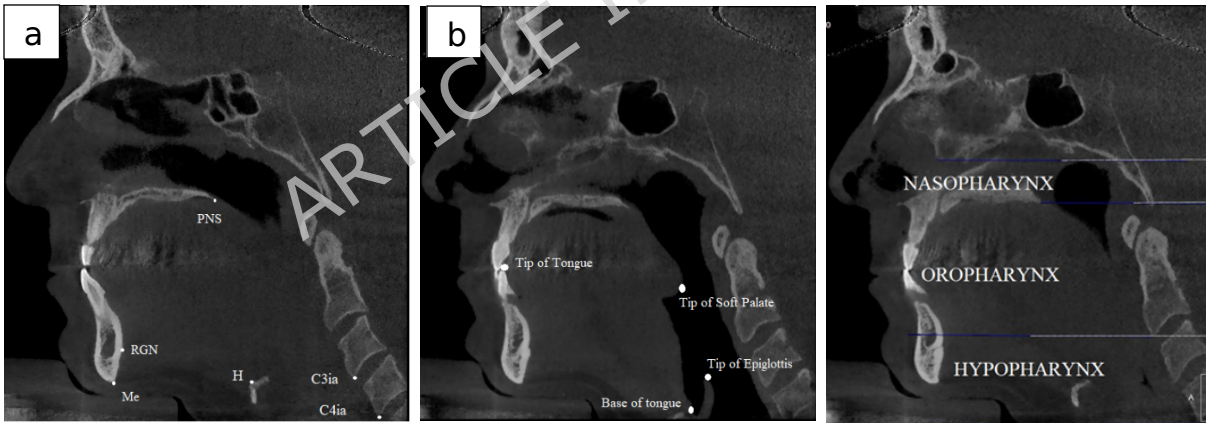

c**. 1.** Landmarks used in this study: (a) hard tissue landmarks, (b) soft tissue landmarks, and (c) outlining the upper airway sub regions in the sagittal plane.

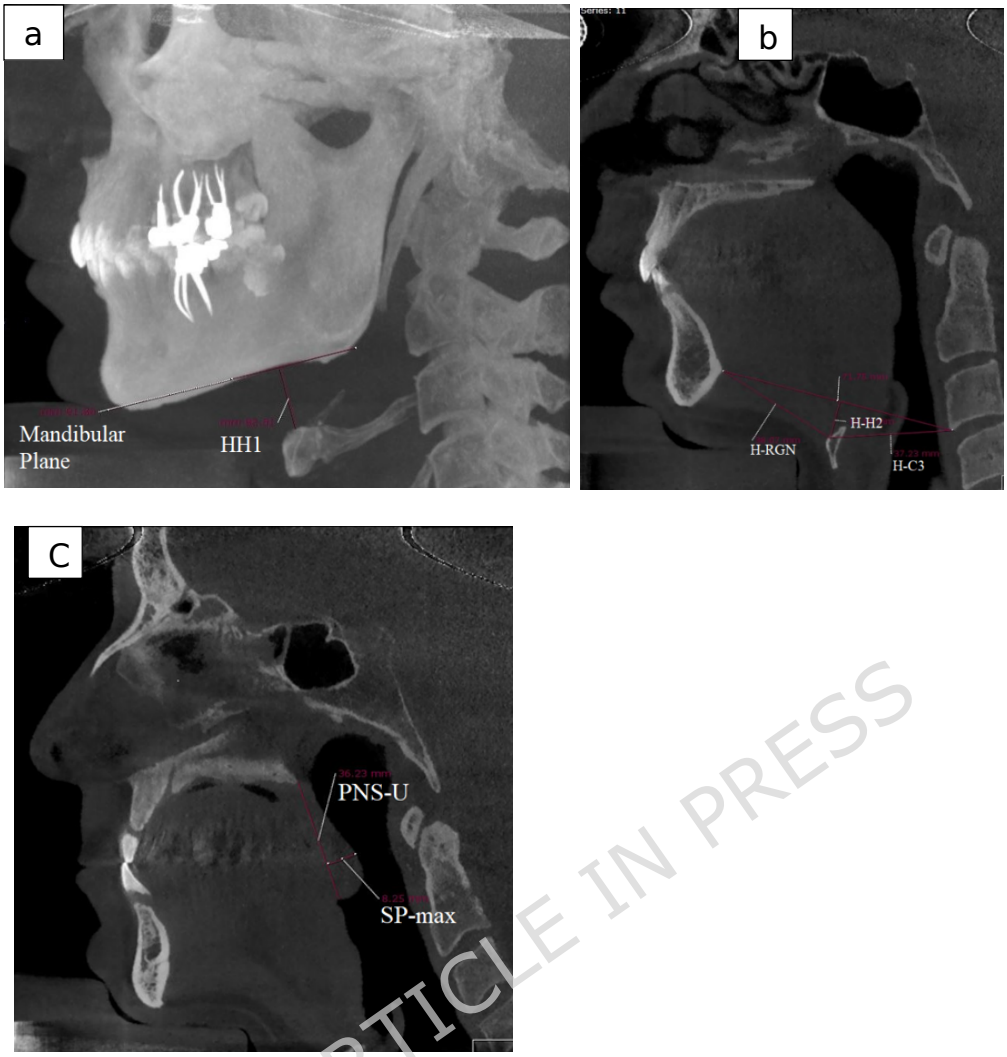

Fig. 2. Measurements on CBCT images using OnDemand software. (a–b) Hyoid bone position assessed in vertical and horizontal dimensions. Vertical measurements included HH1, HH2, and HH1+HH2:
(a) HH1, defined as the linear distance measured along a perpendicular from the hyoid to the mandibular plane (MPH). (b) HH2, defined as the linear distance between the hyoid and a perpendicular to the RGN-C3ia plane (a plane connecting the most inferior-anterior point of the body of the third cervical vertebra to the most inferior-posterior point of the mandibular symphysis). Horizontal measurements in (b) included H–C3ia (the distance between the hyoid and the most inferior-anterior point of the third cervical vertebra) and H–RGN (the distance between the hyoid and retrognathion). (c) Soft tissue measurements, including PNS–U (distance from the posterior nasal spine to the tip of the uvula, representing soft palate length) and SP-max (maximum thickness of the soft palate measured perpendicular to the PNS–U line).

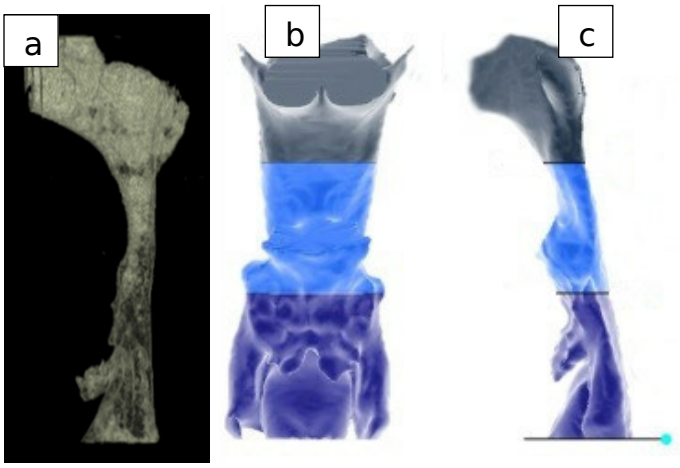

Fig. 3. Airway assessment on CBCT images using OnDemand software, including segmentation and volumetric analysis using three-dimensional reconstruction.
(a) Total airway volume, (b) segmentation of the airway into three regions: nasopharynx, oropharynx, and hypopharynx in the anteroposterior view, (c) lateral view.

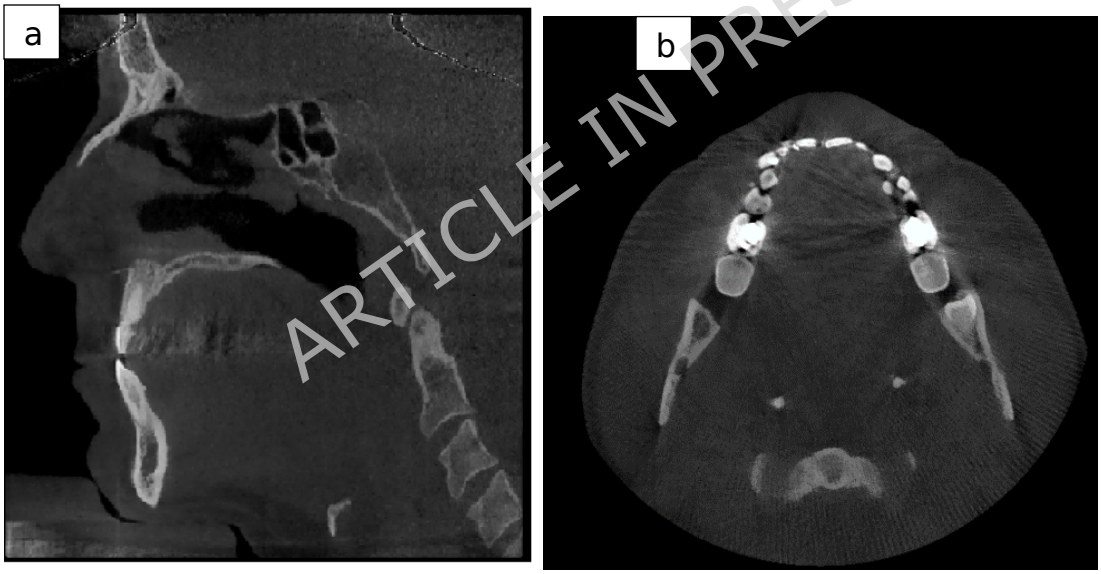

Fig. . CBCT images of a representative patient during the Muller maneuver (a) sagittal view (b) axial view of the same patient.

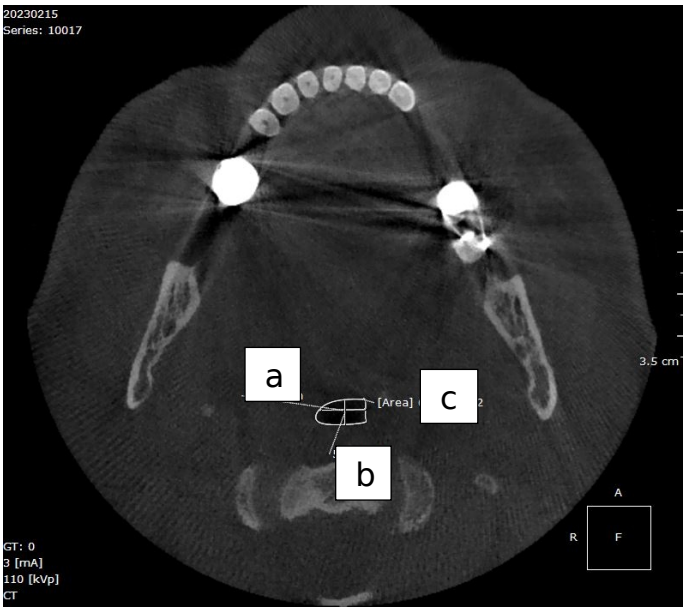

Fig. 5. Airway measurements in the axial section at the level of the narrowest airway segment, identified in the sagittal plane and confirmed in the coronal and axial views. (a) Minimum transverse dimension (mT), (b) minimum anteroposterior dimension (mAP), (c) minimum cross-sectional area (mCSA).

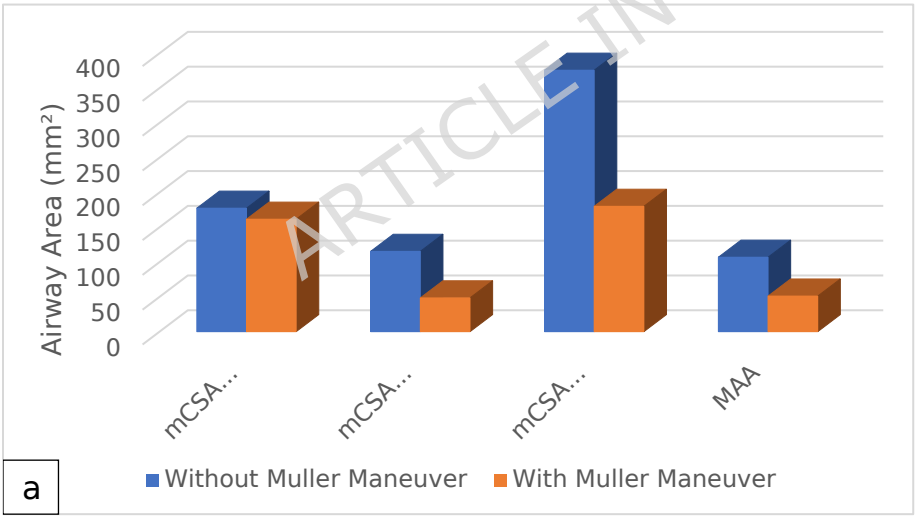

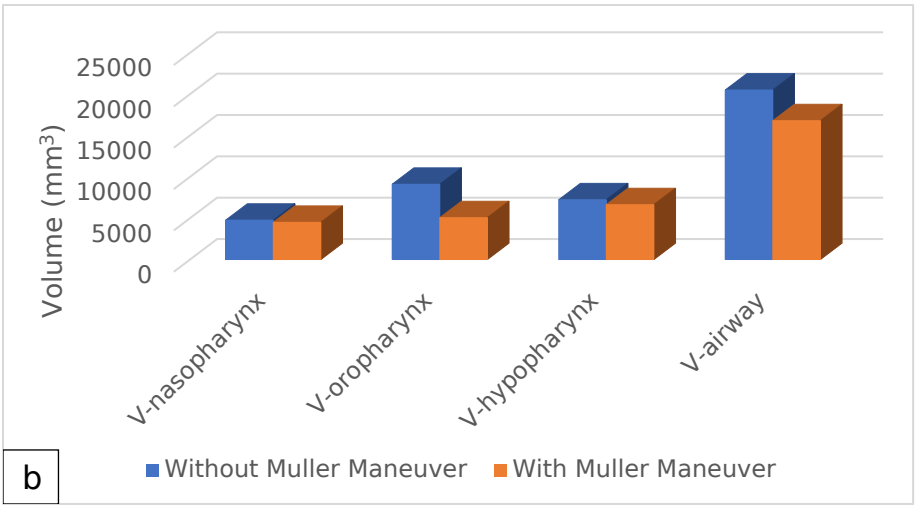

Fig. 6. Effect of the Muller maneuver on upper airway parameters, including minimum cross-sectional area (a) and airway volume (b), evaluated in each subregion (nasopharynx, oropharynx and hypopharynx) as well as the toral airway. (Abbreviations: mCSA, minimum cross-sectional area; MAA, minimum axial area; V, volume)

Figures:

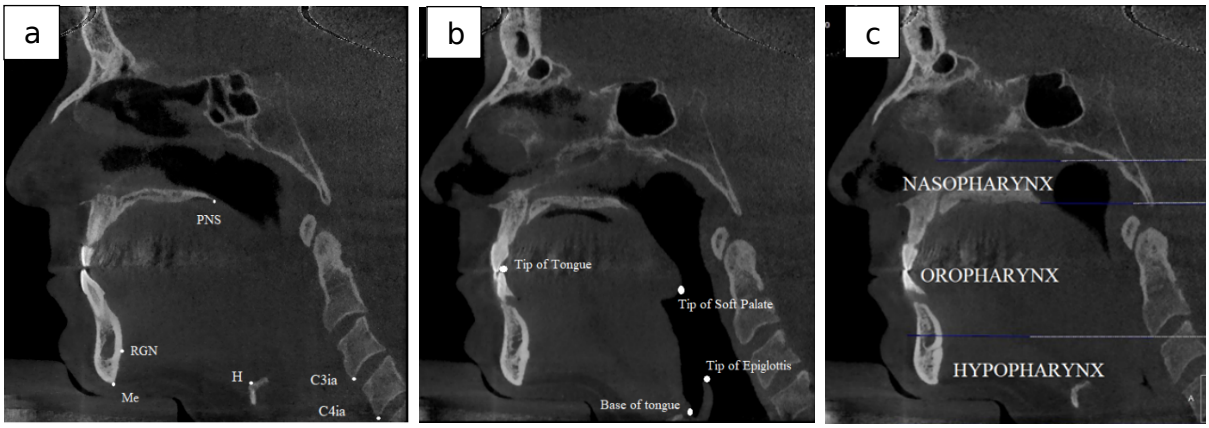

Fig. 1. Landmarks used in this study: (a) hard tissue landmarks, (b) soft tissue landmarks, and (c) outlining the upper airway sub regions in the sagittal plane.

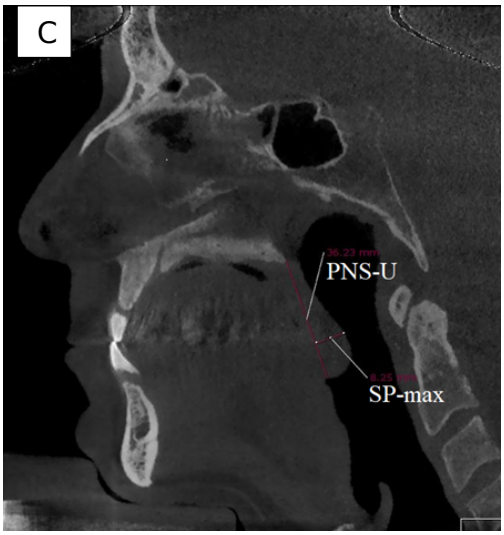

Fig. 2. Measurements on CBCT images using OnDemand software. (a–b) Hyoid bone position assessed in vertical and horizontal dimensions. Vertical measurements included HH1, HH2, and HH1+HH2:
(a) HH1, defined as the linear distance measured along a perpendicular from the hyoid to the mandibular plane (MPH). (b) HH2, defined as the linear distance between the hyoid and a perpendicular to the RGN-C3ia plane (a plane connecting the most inferior-anterior point of the body of the third cervical vertebra to the most inferior-posterior point of the mandibular symphysis). Horizontal measurements in (b) included H–C3ia (the distance between the hyoid and the most inferior-anterior point of the third cervical vertebra) and H–RGN (the distance between the hyoid and retrognathion).
(c) Soft tissue measurements, including PNS–U (distance from the posterior nasal spine to the tip of the uvula, representing soft palate length) and SP-max (maximum thickness of the soft palate measured perpendicular to the PNS–U line).

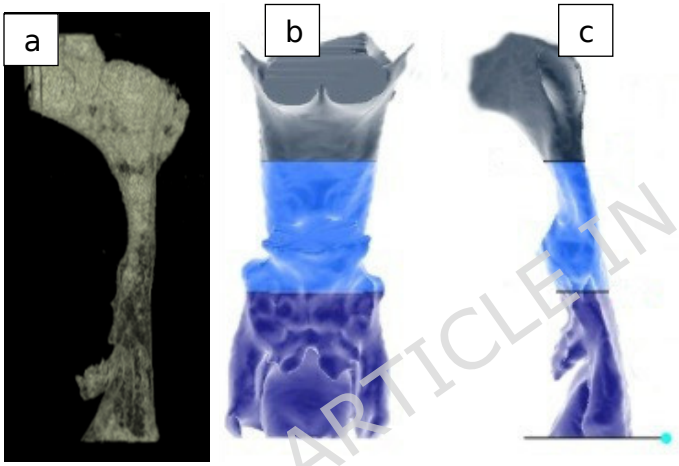

Fig. 3. Airway assessment on CBCT images using OnDemand software, including segmentation and volumetric analysis using three-dimensional reconstruction.
(a) Total airway volume, (b) segmentation of the airway into three regions: nasopharynx, oropharynx, and hypopharynx in the anteroposterior view, (c) lateral view.

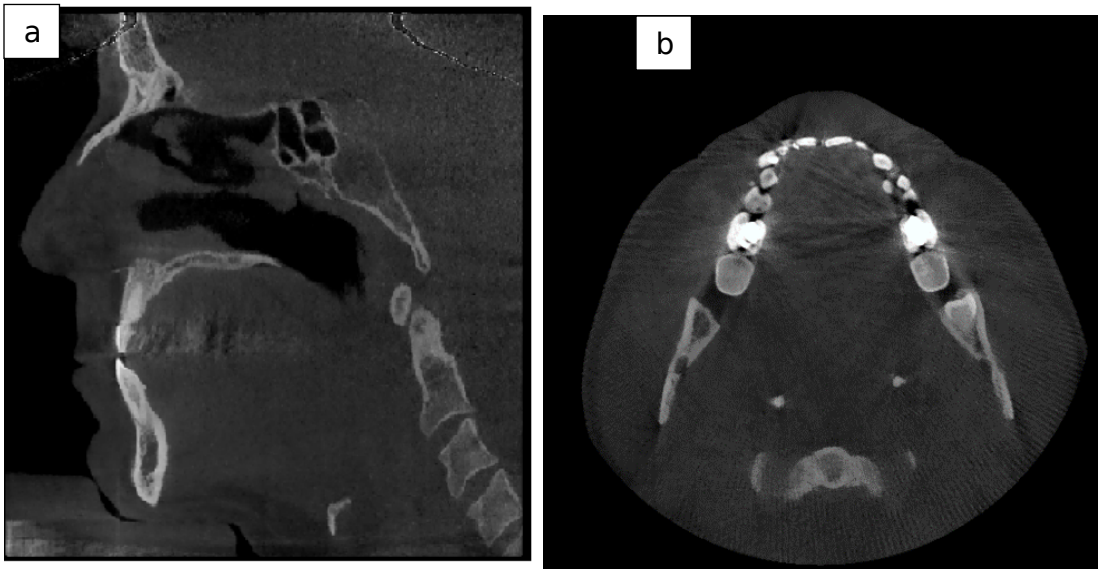

Fig. . CBCT images of a representative patient during the Muller maneuver (a) sagittal view (b) axial view of the same patient.

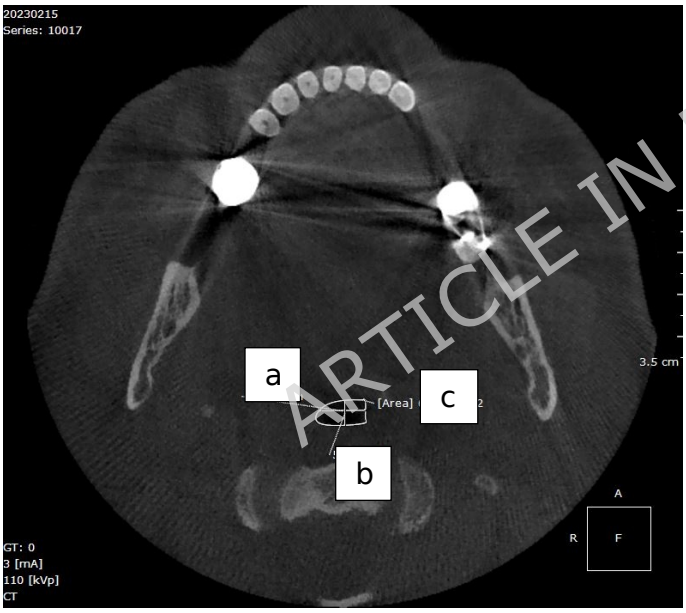

Fig. 5. Airway measurements in the axial section at the level of the narrowest airway segment, identified in the sagittal plane and confirmed in the coronal and axial views. (a) Minimum transverse dimension (mT), (b) minimum anteroposterior dimension (mAP), (c) minimum cross-sectional area (mCSA).

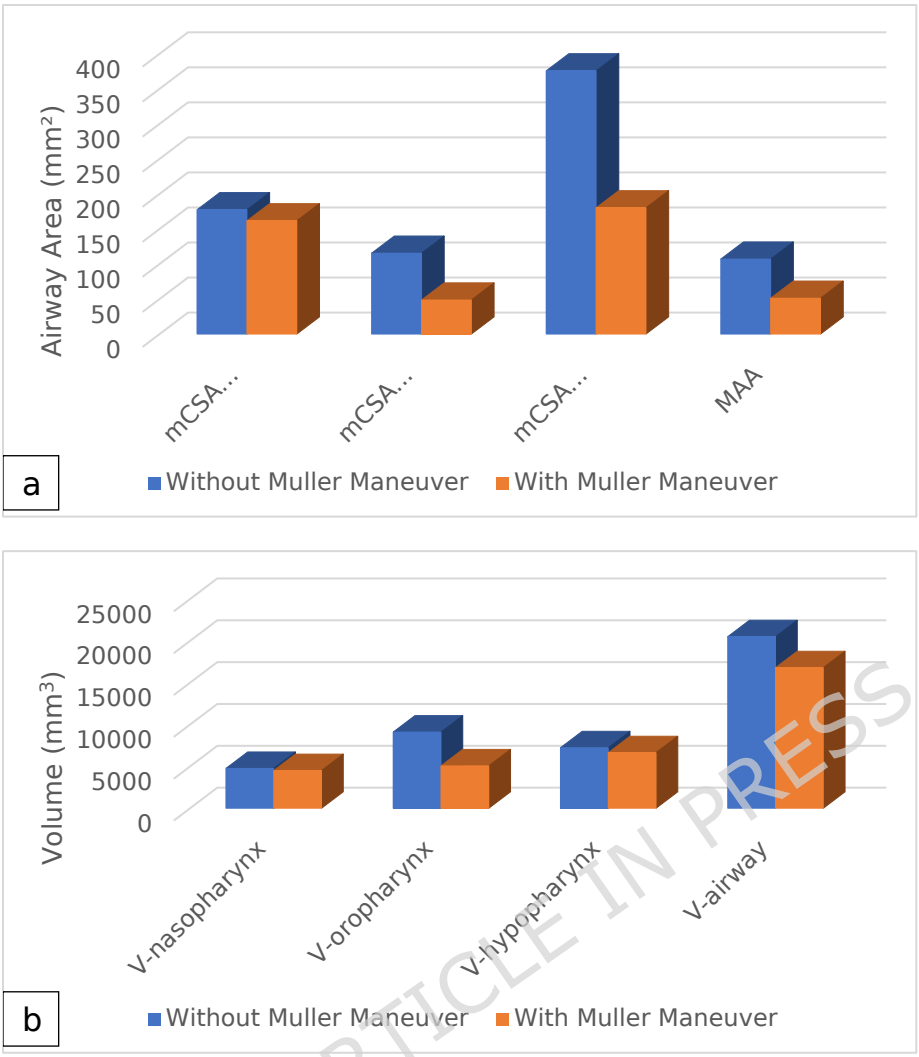

Fig. 6. Effect of the Muller maneuver on upper airway parameters, including minimum cross-sectional area (a) and airway volume (b), evaluated in each subresion (nasopharynx, oropharynx and hypopharynx) as well as the toral airway. (Abbreviations: mCSA, minimum cross-sectional area; MAA, minimum axial area; V, volume)

Tables

Landmark	**Definition**
PNS	Posterior nasal spine: The tip of the posterior nasal spine
Me	Menton: The lower most point on the mandibular symphysis in the midline
Go	Gonion: The intersection of the line connecting the most distal aspect of the condyle to the distal border of the ramus and the mandibular plane
RGN	The most inferior-posterior point on the mandibular symphysis.
C3ia	The most inferior-anterior point of the body of the third cervical vertebra
C4ia	The most inferior-anterior point of the body of the fourth cervical vertebra
H	The upper edge of the frontal area of hyoid body
H1	Perpendicular from H to the mandibular plane (Go-Me)
H2	Perpendicular from H to the line RGN-cv3ia
Linear	**Definition**

Measurements	
FHP	Frankfurt horizontal plane: The line through point Or and Po.
MP	Mandibular plane: The line connecting Me to Go.
HH1	The linear distance along a perpendicular from hyoid (H) to the Mandibular plane: MPH
HH2	The linear distance between hyoid (H) and a perpendicular to the RGN-C3ia plane
HH1+HH2	Vertical hyoid position
H-C3ia	The linear distance between the hyoid (H) and the most inferior-anterior point of the body of the third cervical vertebra
H-RGN	The linear distance between hyoid (H) and retrognathion
PNS-U distance	The posterior nasal spine to the tip of the uvula, which provides a measure of the length of the soft palate.
SP-max	Maximum thickness of the soft palate perpendicular to PNS-U
TGL	Tongue length: the distance from epiglottis base and tongue tip

TGH	Tongue height: the length of the vertical bisector from the dorsal tongue surface to a line connecting between the epiglottis base and tongue tip
mAP	Minimum Anterior Posterior dimension: anteroposterior dimension of the narrowest segment of each subregion
mT	Minimum transverse dimension: transverse dimension of the narrowest segment of each subregion
L-UA	Length of upper airway: the vertical distance from the upper limit of the nasopharynx to the lower margin of the hypopharynx in the mid-sagittal plane
Area measurements	**Definition**
mCSA	Minimum cross-sectional area: cross sectional area of the narrowest segment of each subregion
Volumetric measurements	**Definition**
V-subregion	Volume of each subregion of airway: nasopharynx, oropharynx, hypopharynx

V-UA	volume of upper airway: total volume from the upper limit of the nasopharynx to the lower margin of the hypopharynx in the mid-sagittal plane.

Table 1. Definitions of anatomical landmarks,linear and volumetric measurements used in this study.

Region	**limits**	**Anatomical**	**Technical**
Nasopharynx	Anterior	Frontal plane perpendicular to FH passing through PNS	Same as anatomical
	Posterior	Soft tissue contour of the pharyngeal wall	Frontal plane perpendicular to FH passing through C2sp
	Upper	Soft tissue contour of the pharyngeal wall	Top of the upper airway: Plane parallel to FH passing through the last axial slice before the nasal septum fused with the posterior pharyngeal wall

	Lower	Plane parallel to FH passing through PNS and extended to the posterior wall of the pharynx	Same as anatomical
	Lateral	Soft tissue contour of the pharyngeal wall	Sagittal plane perpendicular to FH passing through the lateral walls of the maxillary sinus
Oropharynx	Anterior	Frontal plane perpendicular to FH passing through PNS	Same as anatomical
	Posterior	Soft tissue contour of the pharyngeal wall	Frontal plane perpendicular to FH passing through C2sp
	Upper	Lower limit of Nasopharynx	Same as anatomical
	Lower	Plane parallel to FH plane passing through C3ai	Same as anatomical
	Lateral	Soft tissue contour of the pharyngeal wall	Sagittal plane perpendicular to FH passing through the

			lateral walls of the maxillary sinus
Hypopharynx	Anterior	Frontal plane perpendicular to FH passing through PNS	Same as anatomical
	Posterior	Soft tissue contour of the pharyngeal wall	Frontal plane perpendicular to FH passing through C2ia
	Upper	Lower limit of Oropharynx	Same as anatomical
	Lower	Plane parallel to FH connecting the base of the epiglottis to the entrance to the esophagus	Plane parallel to FH connecting the base of the epiglottis to C4ai
	Lateral	Soft tissue contour of the pharyngeal wall	Sagittal plane perpendicular to FH passing through the lateral walls of the maxillary sinus
Upper airway	Anterior	Frontal plane perpendicular to FH passing through PNS	Same as anatomical

	Posterior	Soft tissue contour of the pharyngeal wall	Frontal plane perpendicular to FH passing through C2sp
	Upper	Soft tissue contour of the pharyngeal wall	Top of the upper airway: Plane parallel to FH passing through the last axial slice before the nasal septum fused with the posterior pharyngeal wall
	Lower	Plane parallel to FH connecting the base of the epiglottis to the entrance to the esophagus	Plane parallel to FH connecting the base of the epiglottis to C4ai
	Lateral	Soft tissue contour of the pharyngeal wall	Sagittal plane perpendicular to FH passing through the lateral walls of the maxillary sinus

Table 2. Definitions of anatomical boundaries and segmentation criteria used for airway measurements.

Variables (with/without MM)		Mean	Std. Deviation	Unit	P value
Pair 1	H-H1 +	13.1839	5.60066	mm	0.002*
	H-H1 -	18.8322	6.17667	mm	
Pair 2	H-H2 +	7.0383	3.28134	mm	< 0.001*
	H-H2 -	12.2906	4.85505	mm	
Pair 3	(HH1+HH2) +	20.2222	8.33380	mm	0.001*
	(HH1+H2) -	31.1228	10.47617	mm	
Pair 4	H-C3 +	38.3706	4.13488	mm	0.202*
	H-C3 -	37.1861	3.49543	mm	
Pair 5	H-RGN+	41.0350	5.11893	mm	0.031*
	H-RGN -	43.6900	7.25449	mm	
Pair 6	PNS-U +	34.7756	5.77355	mm	0.016*
	PNS-U -	37.8944	6.19687	mm	
Pair 7	SP-max +	7.2094	1.67494	mm	0.061*
	SP-max -	8.18883	1.798669	mm	
Pair 8	TGL +	80.9406	7.56098	mm	0.454*
	TGL -	81.9422	5.28552	mm	
Pair 9	TGH +	39.4522	4.21773	mm	0.194*
	TGH -	40.9894	3.07323	mm	

Pair 10	V-nasopharynx +	4501.3711	1097.88522	mm^3	0.138*
	V-nasopharynx -	4758.8983	1253.12980	mm^3	
Pair 11	V-oropharynx +	5064.4333	2797.54536	mm^3	0.002†
	V-oropharynx -	9101.8544	8441.23895	mm^3	
Pair 12	V-hypopharynx+	6637.9000	2960.02871	mm^3	0.286†
	V-hypopharynx -	7227.1761	3093.65010	mm^3	
Pair 13	V-airway+	16792.9806	5937.45190	mm^3	0.048†
	V-airway-	20498.6528	9288.06575	mm^3	
Pair 14	mCSA nasopharynx+	161.5700	38.90478	mm^2	0.085†
	mCSA nasopharynx-	177.3828	55.28774	mm^2	
Pair 15	mAP-nasopharynx +	6.9606	2.18565	mm	0.048†
	mAP-nasopharynx -	7.5017	1.77169	mm	
Pair 16	mT-nasopharynx +	20.0572	2.73341	mm	0.995*
	mT-nasopharynx -	20.0594	2.63069	mm	
Pair 17	AP/T nasopharynx +	.3505	.11033	mm	0.214*
	AP/T nasopharynx -	.3766	.08166	mm	
Pair 18	mCSA oropharynx+	48.5422	45.42736	mm^2	0.011*
	mCSA oropharynx -	115.3822	77.16149	mm^2	
Pair 19	mAP-oropharynx +	3.9989	3.45455	mm	0.006*
	mAP-oropharynx -	6.7833	2.00536	mm	

Pair 20	mT-oropharynx +	8.9011	7.89603	mm	0.006*
	mT-oropharynx -	18.1906	7.50047	mm	
Pair 21	AP/T oropharynx +	.4059	.51180	mm	0.145†
	AP/T-oropharynx -	.4331	.21656	mm	
Pair 22	mCSA Hypopharynx +	180.1044	82.87810	mm^2	0.048†
	mCSA Hypopharynx -	375.6239	588.32984	mm^2	
Pair 23	mAP hypopharynx +	8.7106	4.43909	mm	0.039†
	mAP hypopharynx -	12.0417	3.78838	mm	
Pair 24	mT hypopharynx +	19.4922	9.74157	mm	0.070*
	mT hypopharynx -	25.0512	8.41106	mm	
Pair 25	AP/Thypopharynx +	.5380	.38627	mm	0.501†
	AP/T hypopharynx -	.5441	.30298	mm	
Pair 26	MAA in airway +	51.1344	51.81048	mm^2	0.007†
	MAA in airway -	106.9567	50.10624	mm^2	
Pair 27	Airway length +	89.1472	6.01096	mm	0.123*
	Airway Length -	89.8411	6.72913	mm	

Table 3. Comparison of variables obtained from CBCT images with and without the Muller maneuver.

Abbreviations: +, with Muller maneuver; -, without Muller maneuver; AP, Anteroposterior; T, transverse; AP/T, anteroposterior/transverse; V, volume; mCSA, minimum cross-sectional area; MAA, minimum axial area; * based on paired t-test; † based on Wilcoxon signed rank test

Variable	Minimum	Maximum	Mean	Std. Deviation	Cohen's d
H-H1 change	-75.08	19.90	-27.4352	27.90261	0.98
HH2 change	-78.84	6.14	-37.0960	27.52064	1.35
HH1+HH2 change	-76.60	11.05	-31.8108	25.39856	1.25
H-RGN change	-20.33	14.04	-5.0734	10.14688	0.50
PNS-U change	-33.54	8.99	-7.5154	11.39206	0.66
V-oropharynx change	-94.24	27.85	-27.4168	33.83232	0.81
V-airway change	-76.80	14.41	-11.7620	22.98114	0.51
mAP-nasopharynx change	-35.49	59.16	-6.4133	23.60183	0.27
mCSA-oropharynx change	-100.00	83.93	-42.0299	60.00345	0.70
mAP-oropharynx change	-100.00	79.30	-38.8182	52.94263	0.73
mT-oropharynx change	-100.00	40.90	-38.8803	52.72732	0.74
mCSA-hypopharynx change	-100.00	126.65	-11.7782	60.61004	0.19
mAP-hypopharynx change	-100.00	36.58	-19.7762	38.77550	0.51
MAA change	-100.00	93.07	-39.0139	64.65082	0.60

Table 4. Statistical measures and effect sizes for variables demonstrating statistically significant differences following the Muller maneuver.